Melody Khoriaty and Finn Bergquist

Interrupted two-dimensional flow modeled using successive overrelaxation

Introduction:

When fluid flows around a stationary object, laminar streamlines must divert to circumvent the obstruction. The fluid will do this in different ways based upon its velocity and viscosity. When the fluid has certain parameters, it will create an eddy on the downstream side of the object - an area where the fluid flows in the opposite direction of the free stream flow, filling in the space around the object from the downstream side instead of the upstream side.

Such a system can be modelled using successive overrelaxation (SOR). In two dimensions and for an incompressible fluid, this can be done using the equations for the stream function Ψ:

$$\nabla^2\Psi = -\,\omega$$

and for vorticity ω:

$$\nabla^2\omega = \frac{1}{v}\left(\frac{\partial\Psi}{\partial y}\frac{\partial\omega}{\partial x} - \frac{\partial\Psi}{\partial x}\frac{\partial\omega}{\partial y}\right).$$

Here we attempt to simulate viscous, incompressible, two-dimensional flow around a stationary obstruction using an SOR method.

Methods:

We initialized two square vertex-centered matrices with dimensions of 64x64, one to contain values of the stream function, Ψ and the other having values of vorticity, ω. The vorticity matrix had all values initialized to zero, while the stream function matrix had three boundaries initialized to zero and all other points initialized as

$$uyg$$

where u is the initial velocity, y is the y coordinate, and g is the grid spacing. In addition, an obstruction - a “plate” or an area of no flow - was set within the bounds of the matrix.

To perform one sweep, both Ψ and ω values were updated for each coordinate based on the surrounding points. At interior points, Ψ was updated to be the average of surrounding points and ω was updated to be

$$\frac{1}{4}\left(n_s - \frac{g^2}{v}\left(\frac{d\Psi}{dy}\frac{d\omega}{dx} - \frac{d\Psi}{dx}\frac{d\omega}{dy}\right)\right)$$

with n_s being the sum of the four surrounding values, g being the grid spacing, and v being viscosity. Boundary conditions on the top and bottom were maintained at zero for omega, as were upstream omega values. The top boundary condition for psi was

$$\Psi_l + ug$$

where Ψ_l is the Ψ value of the point directly below it in the y direction. Upstream and downstream psi values, and downstream omega values, were set to the same value as the points immediately down- or upstream. Points within the plate were maintained at 0. Psi values on the sides of the plate were maintained at 0. Omega values on the upstream, downstream, and upper sides of the plate were set to

$$\frac{-2}{g^2}\Psi_n$$

where Ψ_n is the Ψ value closest to it on the side towards the flow.

The residual of Ψ was calculated as the sum of the second derivatives in both the x and y direction. Sweeps were repeated until the square root of the sum of the squares of the residuals (the norm) for the matrix reached an arbitrarily low value.

Results:

A contour plot of the stream function with a viscosity of 0.1 until the norm was less than 300 shows that fluid flow diverges around a stationary object, with an area of influence near to the object where flow changes direction most sharply and where the velocity gradient is more pronounced (Figure 1). Further from the object streamlines do not change course as significantly. When compared to a contour plot with a viscosity an order of magnitude lower, it can be seen that, with all other parameters equal, a lower viscosity also creates an eddy on the downstream side of the object, where flow moves in the negative direction - ie from downstream towards the upstream object (Figure 1, 2c).

Contour plots of Ψ with varying required norms show how the stream functions change as the standards for the tolerance are increased (Figure 2). While larger matrices cannot achieve the same norm (due to a lack of computing power available), it can be seen that as the norm is decreased the eddy increases in length and decreases in speed. The streamlines further from the obstruction also diverge slightly more as the norm decreases: ie, they are directed more upward near the top of the matrix.

With an increase in matrix size the eddy decreases in length but has more negative flow (ie flow with a higher speed in the negative direction) for a similar number of sweeps (Figure 2).

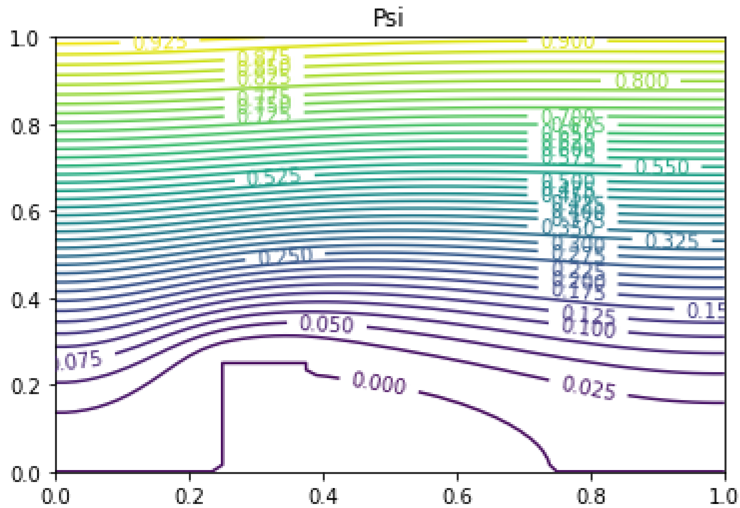

Figure 1: Contour plot of Ψ with a matrix size of 64. Sweeps were repeated until the norm was less than 100. Viscosity was set to 0.1 and initial velocity to 1.

Matrix size - 64	Matrix size - 99
a. Norm < 500 (sweeps: 47) 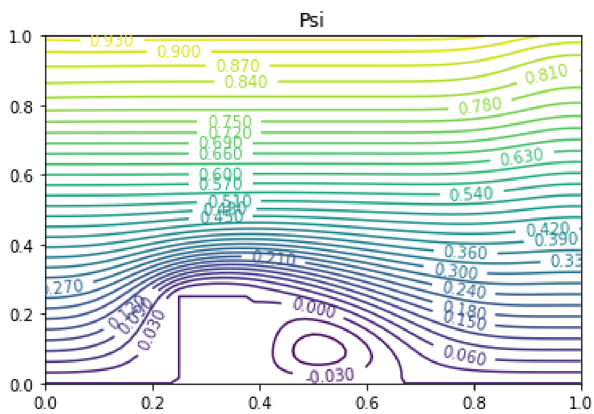	d. Norm <1000 (sweeps: 66) 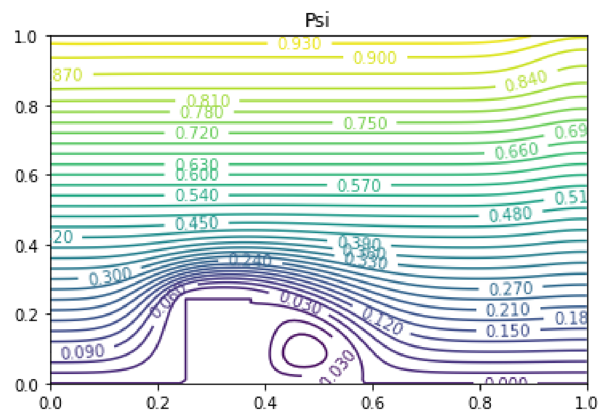
b. Norm <300 (sweeps: 113) 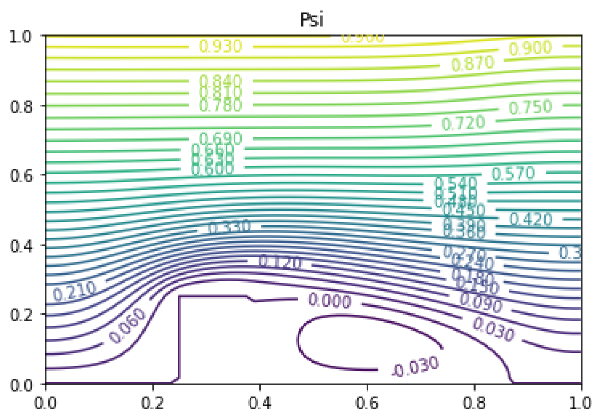	e. Norm <300 (sweeps: 418) 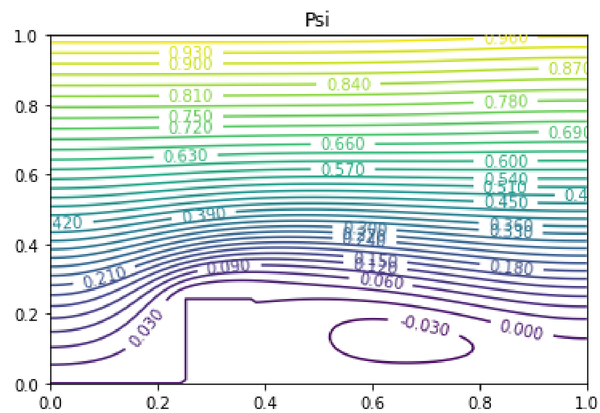
c. Norm <100 (sweeps: 376) 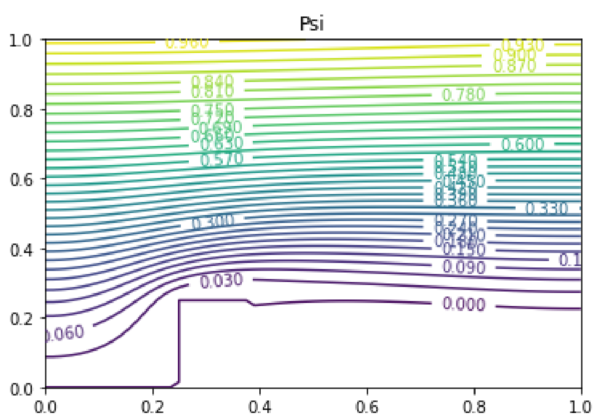	f. Norm <100 (sweeps: 1668) 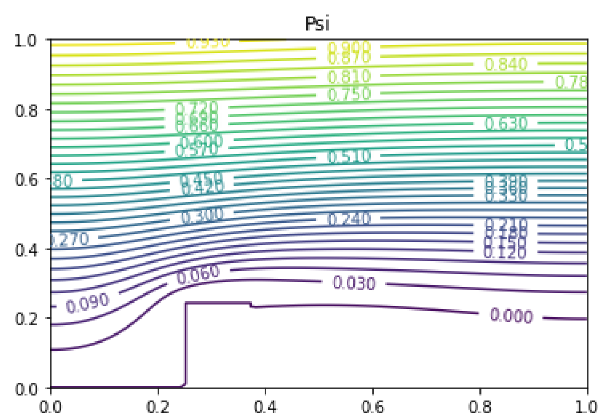

Figure 2: Contour plots of Ψ with varying matrix sizes until varying norms have been achieved. All plots have a viscosity of 0.03 and an initial velocity of 1.

Discussion:

This numerical model corresponds somewhat with real-world fluid flow states, where obstructions can create an eddy if the Reynold's number is sufficiently high/viscosity is sufficiently low. However, there are only limited cases in which it can be useful, as in its current form it does not include a flexible interface between the fluid and a surrounding environment. When a fluid (such as water) passes an obstruction (such as a rock in a stream), it can change in thickness (ie a hydraulic jump). This behavior is based on the Froude number, $Fr = \frac{u}{\sqrt{gh}}$, where h represents the characteristic depth of the fluid (although in non-uniform flows this can be different) (Waltham, 2004). This current model does not have an upper interface, and therefore cannot model hydraulic jumps or thickening/thinning of the fluid; it instead models a fluid as if it is wholly contained. While this is true for systems like pipes, it is not the case for most geomorphological systems such as streams or air currents.

This model also inherently assumes exclusively laminar flow and does not depict boundary layers. While laminar flow is present for a certain range of Reynold's numbers ($Re<5x10^5$), at higher Reynold's numbers turbulence arises. Both laminar and turbulent conditions are critical for any understanding of how fluid flow affects most biological systems, from fishways in dams (Gisen et al, 2017) to oxygen and nutrient diffusion (Higashino and Stefan, 2005). While boundary layers can seem quite small to humans, a 0.5-3.5 mm layer (as has been measured on the seafloor) becomes very important to small benthic organisms (Archer et al 1989). Juvenile barnacles are often only 0.5 mm in size, and other benthic organisms such as corals exist along a similar scale (Hoffman 1984). This SOR model, therefore, is useful for larger-scale fluid patterns (such as the presence of eddies, and differences in flow based on viscosity) but has limitations at small scales or in environments with less defined boundaries.

References:

Archer, D., Emerson, S., & Smith, C. R. (1989). Direct measurement of the diffusive sublayer at the deep sea floor using oxygen microelectrodes. *Nature*, *340*(6235), 623-626.

Gisen, D. C., Weichert, R. B., & Nestler, J. M. (2017). Optimizing attraction flow for upstream fish passage at a hydropower dam employing 3D Detached-Eddy Simulation. *Ecological Engineering*, *100*, 344-353.

Higashino, M., & Stefan, H. G. (2005). Sedimentary microbial oxygen demand for laminar flow over a sediment bed of finite length. *Water research*, *39*(14), 3153-3166.

Hoffman, D. L. (1984). Size-frequency distribution patterns of the juvenile stages of the pendunculate barnacle, *Pollicipes polymerus* Sowerby, 1833 (Cirripedia, Lepadomorpha). *Crustaceana*, 295-299.

Waltham, D. (2004). Flow transformations in particulate gravity currents. *Journal of Sedimentary Research*, *74*(1), 129-134.